Quantum efficiency decay mechanism of NEA GaN photocathode: A first-principles research

Yang Shen (沈 洋)[1,*], Liang Chen (陈 亮)[1,2,], Shuqin Zhang (张淑琴)[1], and Yunsheng Qian (钱芸生)[2]**

[1]*Institute of Optoelectronics Technology, China Jiliang University, Hangzhou 310018, China*

[2]*School of Electronic and Optical Engineering, Nanjing University of Science and Technology, Nanjing 210094, China*

**Corresponding author: 920778028@qq.com; **corresponding author: LChen@cjlu.edu.cn*

Received June 12, 2015; accepted July 31, 2015; posted online September 8, 2015

Using the first-principles method based on the density functional theory (DFT), the work function of seven different GaN (0001) (1×1) surface models is calculated. The calculation results show that the optimal ratio of Cs to O for activation is between 3:1 and 4:1. Then, Cs/O activation and stability testing experiments on reflection-mode negative electron affinity GaN photocathodes are performed. The surface model [GaN (Mg): Cs] Cs-O after being activated with cesium and oxygen is used. The experiment results illustrate that the adsorption of O contained in the residual gas increases the surface potential barrier and the reduction of the effective dipole quantity is the basic cause of the quantum efficiency decay.

OCIS codes: 040.7190, 160.1890, 230.0040, 260.7210.

doi: 10.3788/COL201513.100401.

With the rapid development of lithographic manufacturing and ultraviolet (UV) detection technology, a high performance UV photocathode is urgently needed[1–5]. A GaN-based photocathode is a new type of semiconductor material with the excellent characteristics of wide bandgap, low dielectric constant, corrosion resistance, high temperature resistance, and radiation resistance, so it has recently gained much interest among those who wish to use it in high power, optoelectronic, and microelectronic devices[6–8]. It has become an attractive candidate due to its stable physical and chemical properties, high quantum efficiency (QE), low dark current, and concentrative emitting electron energy distribution[9–11]. Because of the wide bandgap, GaN photocathodes are naturally "solar blind" and do not respond to visible light, so they have plenty of uses in the fields of UV detection, fire alarm technology, atmospheric monitoring, lithographic manufacture, and others. These areas require not only higher sensitivity and good emission properties but also the stability of the QE of the cathode. But the practical application has encountered a number of obstacles; the most important is a stable GaN photocathode in a vacuum system in nature, that is, the QE of the GaN photocathode attenuation problem in a vacuum system. To take full advantage of the excellent properties of a negative electron affinity (NEA) GaN photocathode, it is essential for researchers to study the reason for the QE decay, and thus improve its stability.

A GaN photocathode activated by Cs/O can reach a higher QE because of the NEA[12–16], but after a while the adsorption of residual gases such as oxygen in a demountable vacuum system can act on the activated NEA surface and influence photocathode stability. How to well analyze the QE decay mechanism of the NEA GaN photocathode further becomes the important part of our study, and only knowing the reason why it declines can we better improve the QE of the photocathodes. From the studies of the NEA GaAs photocathode it can be found that the QE mainly depends on the performance of the material and the technique of preparation[17]. Wang *et al.* have studied the influence of the p-type doping concentration on the GaN photocathode, and the optimal concentration has been found[18]. In this Letter, we investigated and discussed the influence of residual gas on the QE after activation and optimized the preparation technology of the NEA GaN photocathode.

Calculations in this Letter are performed with the quantum mechanics program Cambridge Serial Total Energy Package (CASTEP) code[19]. The generalized-gradient approximation (GGA) parameterized by Perdew–Burke–Ernzerhof (PBE) is adopted to calculate the exchange-correlation energy. The Broyden–Fletcher–Goldfarb–Shanno (BFGS) algorithm[20–22] is used to relax the structure of the crystal model[23]. All calculations are carried out in reciprocal space and the atomic pseudopotentials, described by the ultra-soft pseudopotential, are generated from the following electronic configurations: Ga:$3d^{10}4s^2 4p^1$, N:$2s^2 2p^3$, Cs:$5s^2 5p^6 6s^1$, O:$2s^2 2p^4$, and H:1s. The convergence parameters are set as follows: energy change below 2×10^6 eV/atom, force less than 0.005 eV/nm, stress less than 0.05 GPa, and change in displacement less than 1×10^5 nm in an iterative process. The Brillouin zone integral is sampled with the Monkhorst–Pack mesh scheme and special k points of high symmetry. After a series of tests, the energy cutoff of the final sets of energies is set as 400 eV and the number of k points[24] for a GaN (0001) surface is set as $6 \times 6 \times 1$.

 © 2015 Chinese Optics Letters

As depicted in Fig. 1, the surface slab models are modelled[23] with six GaN layers to simulate a GaN (0001) (1×1) surface. Seven different adsorption models are built to verify whether the amount of Cs or O is enough for the activation process. To prevent the transfer of surface charges and remove the artificial surface-related quantum states from the vicinity of the Fermi level the dangling bonds on the back surface are saturated with a layer of fractionally charged $(Z = 0.75)$[25] hydrogen-like pseudo atoms. Since the slab model entails the existence of the dipole[25], a self-consistent dipole correction is performed to compensate for the dipole. The top three layers of the GaN (0001) slab model are relaxed freely and the bottom three layers are fixed. A vacuum thickness of 1.5 nm is used to avoid interaction between repeated slabs.

Before starting the surface model calculations we first optimized the clean bulk GaN surface. The lattice parameters using the experimental value can be described by $a = b = 0.3189$, $c = 0.5185$, $\alpha = \beta = 90°$, and $\gamma = 120°$, where $c/a = 1.626$. After optimization, the lattice constants are $a = b = 0.32805$ and $c = 0.50103$, which are in good agreement with the experimental values, indicating the correctness of the current calculation method[26].

Different surface models of (1×1) GaN (0001) were built. Based on first-principle calculations, the adsorptions and work functions were obtained and listed in Table 1.

The adsorption energies E_{ads} of different surface models are all positive, showing that it is an endothermic process and the adsorbed system is not stable. But it can be concluded that model (b), model (e), and model (f) are more relatively stable in energy when compared to other models.

The photoemission of NEA photocathodes is described as a three-step process of optical absorption in a bulk, electron transport from the bulk to the surface, and escape across the surface into a vacuum by Spicer in 1958[27]; the third step mainly depends on the work function. For semiconductors, the work function is defined as the minimum energy that electrons of a crystal require to escape into a vacuum, and can be calculated by[28]

$$\varphi = E_{\text{vacuum}} - E_f, \tag{1}$$

where E_{vacuum} is the energy level of the vacuum and E_f is the Fermi level of every surface. The ionization energy mentioned in Ref. [29] was defined as the energy that the photoelectron needed to escape from the bulk to the vacuum and the work function was defined as the energy difference between the E_{vacuum} and the E_f in Eq. (1). According to the definitions, theoretically, the work function ought to be slightly less than the ionization energy. The ionization energy of the clean undoped GaN surface is 4.9 eV in the experiment. The values of the surface work function are shown in Table 1. The work function value of different surface models is calculated and analyzed. In Table 1, the work function value of the clean GaN (0001) surface is 4.18 eV, which is slightly less than the ionization energy and in keeping with the theory conclusion. Therefore, the calculated values of the work function are reliable.

As shown in Table 1, when one Cs atom is adsorbed on the (1×1) GaN (0001) surface, the calculated work function is 2.52 eV after free relaxation, which is lower than the clean (1×1) GaN (0001) surface mainly because the electronegativity of the Ga atom is larger than that of the Cs atom, and thus the Cs atom is losing electrons that are moving to the Ga atom. Then, another Cs atom is adsorbed on top of the surface of model (b) and the value of the work function is 2.59 eV after relaxation, which rises slightly compared to model (b). The main reason is that with the increase of Cs coverage electrons move from the surface of the Ga atom to the first adsorption layer of the Cs atom, thus causing the surface dipole to slightly increase and further leading to adsorption unstability. On the basis of model (c), one additional oxygen atom is admitted onto the top of the GaN (0001)-Cs-Cs surface; after relaxation, the value of the work function is 6.49 eV, which is 3.9 eV larger than for model (c). This is mainly because the electronegativity of a Cs atom is smaller than that of an O atom, thus the Cs atom losing electrons becomes positive and the O atom obtaining electrons becomes negative, and surface dipole moments form following this interaction. The O atom and the second adsorption Cs atom formed a downward dipole moment, which weakened the original dipole moment, thus causing the work

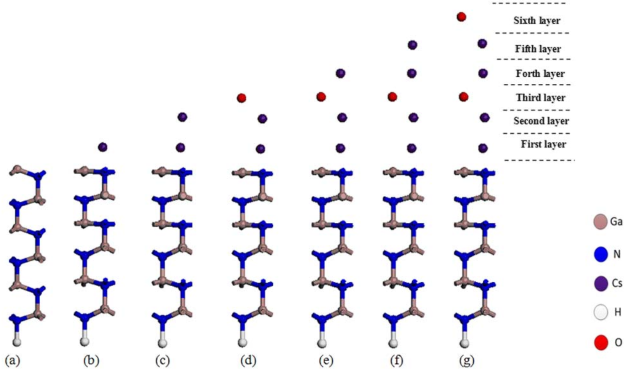

Fig. 1. (a) Clean (1×1) GaN(0001) surface model, (b) GaN (0001)-Cs surface model, (c) GaN(0001)-Cs-Cs surface model, (d) GaN(0001)-Cs-Cs-O surface model, (e) GaN(0001)-Cs-Cs-O-Cs surface model, (f) GaN(0001)-Cs-Cs-O-Cs-Cs surface model, and (g) GaN(0001)-Cs-Cs-O-Cs-Cs-O. The dotted lines indicate the range of each layer.

Table 1. The Calculated Values of Adsorption Energies and Work Functions for Different Surface Models, "+" Means Increment while "−" Means Decrement

Model	a	b	c	d	e	f	g
E_{ads} (eV)		0.36	7.18	9.24	0.18	0.27	2.18
ϕ (eV)	4.18	2.52	2.59	6.49	1.59	1.57	2.46
$\Delta\phi$ (eV)		−1.66	+0.07	+3.90	−4.90	−0.02	+0.89

function to increase. Then, as depicted in model (e), the value of the work function is 1.59 eV, which decreases greatly when compared with model (d); this is mainly because with the superposition of dipole moments a stronger upward dipole moment forms, which results in the work function declining further and, at the same time, the state of NEA forms. On the basis of model (e), model (f) is put forward to verify whether the amount of Cs is enough for the work function declining. The value of model (f) is similar to model (e), indicating that an over-cesiumized atmosphere is formed and the larger amount of Cs atom has little effect on the work function declining, thus affecting the stability of the NEA photocathodes. Finally, another oxygen atom is added on model (f); the results show that the work function increases again, the adsorption of excess O increases the surface potential barrier, and the stability of the activated photocathodes can be thus weakened.

In summary, we can draw the conclusion that the optimal ratio of Cs to O for activation is between 3∶1 and 4∶1, which lowers the work function and promotes photoemission. But excess O modules increase the work function and undermine the photocathode, which is not beneficial for the stability of photocathodes.

Variations of the photocurrent during the Cs/O activation process and the stability of the GaN photocathode are tested and investigated. As depicted in Fig. 2, an activation experiment is performed on a high-quality p-type Mg-doped reflection-mode GaN substrate grown by metal organic chemical vapor deposition (MOCVD). The doping concentrations are 8.66×10^{16} cm^{-3}. After chemical etching by H_2SO_4:H_2O_2:H_2O = 2∶2∶1 for 10 min, the sample was transferred into an ultra-high vacuum (UHV) chamber with a base pressure of less than 1×10^{7} Pa and heated to remove the surface contamination such as carbon and oxides. The heat cleaning was performed on the back side of the sample by thermal irradiation from a halogen tungsten filament lamp and the temperature was measured by a thermocouple. The sample was heated at a temperature of about 710°C for 20 min. When the sample cooled down to room temperature, Cs/O activation was performed in the UHV chamber in which the cesium source was kept continuous and the oxygen source was introduced periodically[30,31]. During the activation process, the photocurrent was controlled and monitored by a multi-information online monitoring system established by ourselves[32,33]. The photocurrent appears after 3 min of activation. The photocurrent increases with the increase of the Cs flux. The value of the photocurrent reaches the first peak (time = 26 min) of 1.55 μA; after the peak value, the photocurrent does not rise again. Then, the O flux enters and the photocurrent begins to rise slightly. The Cs/O activation process ends at the time of 52 min and the photocurrent is still unchanged until the time of 80 min. 80 min later the photocurrent decreases greatly and almost returns to the intrinsic value, which is caused by the UV light source turning off. When we turn on the UV light source again the photocurrent is back to the value of 80 min, indicating that the GaN photocathode has a higher performance with superior stability.

To better understand the QE decay mechanism of the NEA GaN photocathode, the cathode QE curve in situ was tested after the Cs/O activation process completed. Then the sample was placed in a vacuum chamber for 6 h and the QE curve in situ was also tested and compared with the original curve 6 h later. As depicted in Fig. 3, after 6 h of decay there was an overall decline in the QE curves and the QE of the cathode produced a significant attenuation. The short wavelength region dropped down by a smaller amplitude, but the long-wavelength region dropped down by a larger extent. The loss of QE in the short-wavelength region is less than that in the long-wavelength region QE, indicating that with the wavelength increasing the loss of QE increased.

According to the research of Machuca[34], as time went on the QE of the GaN photocathode was in constant attenuation and the QE decreased to 20% of the original value. The main reason for the QE decay is that the degree of vacuum was declining, which is consistent with our experiments.

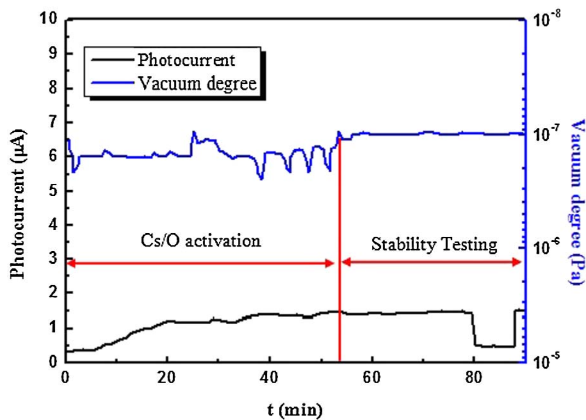

Fig. 2. Variation of the photocurrent during the Cs/O activation process and stability testing of a NEA GaN photocathode.

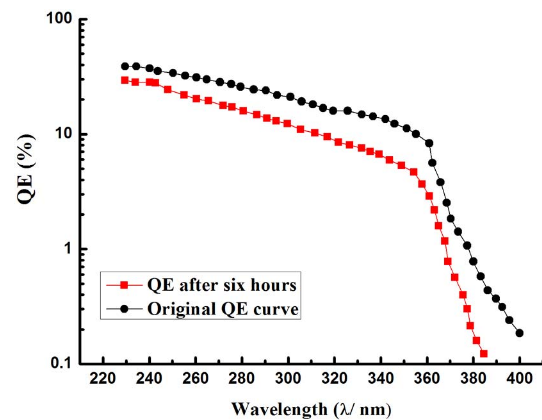

Fig. 3. Variation curves of the QE of a NEA GaN photocathode after 6 h of decay.

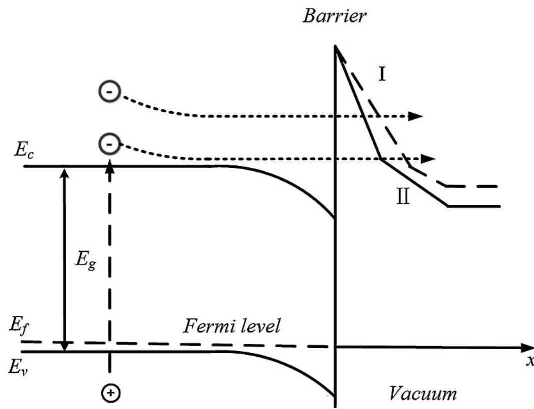

Fig. 4. Schematic surface barrier and energy band variations of an R-mode NEA GaN photocathode before and after decay.

It can be seen from Fig. 4 that the surface barrier changed during the decay process. The surface barrier is composed of two straight lines of different slope. The dipole ([GaN (Mg): Cs]) marked in Fig. 5 formed during the Cs-alone activation process that formed the first barrier (I), and the vacuum level is lowered to NEA state. The introduction of oxygen and the Cs-only dipole layer form a cesium oxide dipole layer, which is called the second barrier (II). The amount and the direction of the [GaN (Mg): Cs] and Cs-O dipoles in the active layer are two essential factors for QE decay. The positive terminal side of the equivalent dipoles points to the vacuum layer, which is a benefit for the electrons escaping from the surface. Combined with the theory calculation results, we can demonstrate the conclusions that excess O modules increased the work function and destroyed the degree of vacuum, which leads to the QE decay[35].

The adsorption of O contained in the residual gas increases the surface potential barrier. By supplying additional Cs flux at the end of the cathode activation process, the degradation rate can be reduced and the stability of the activated photocathodes can thus be enhanced. In addition, according to Ref. [36], the vacuum pressure is crucial and the cathode lifetime can be extended by an order of magnitude if the vacuum pressure is improved by an order of magnitude.

Above all, during the QE decay process, after successful activation the GaN cathode is easily affected by the surrounding impurities, especially oxygen and the oxygen-containing impurities adsorbed on the surface of the active layer. At the same time, the Cs desorption phenomenon in the active layer can also occur. These effects damage the formation of dipoles in the active layer, thus causing the effective electron emitting dipole to decrease greatly. The decreased amount of equivalent dipoles will significantly reduce the QE of the cathode and lead to a decrease in sensitivity.

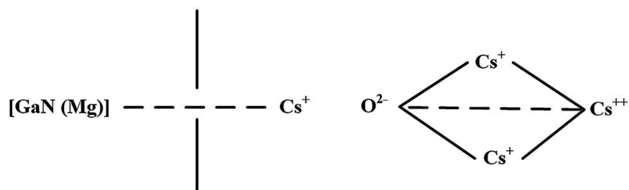

Fig. 5. Formation of a [GaN (Mg): Cs] dipole and a Cs-O dipole.

In conclusion, based on the first-principle density functional theory, seven different adsorption models are built to verify whether the amount of Cs or O is enough for the activation process. The calculation results show that the optimal ratio of Cs to O for activation is between 3∶1 and 4∶1, which lowers the work function and promotes photoemission. Excess O modules increase the work function and undermine the photocathode, which is not beneficial for the stability of photocathodes. Cs/O activation and stability testing experiments on the reflection-mode NEA GaN photocathode are performed. Variations of the photocurrent during the Cs/O activation process and the stability of the GaN photocathode are tested and investigated. The experiment results illustrate that the adsorption of O contained in the residual gas increases the surface potential barrier and the reduction of the effective dipole quantity is the basic reason for QE decay. A combination of theoretical calculation with experimental analysis methods can help to study well and optimize the QE decay mechanism of GaN photocathodes and QE recovery in future research.

The authors would like to thank Meishan Wang of the School of Information and Electrical Engineering, Ludong University for the first principle calculations.

This work was supported by the National Natural Science Foundation of China (Nos. 61308089 and 61440065), the Public Technology Applied Research Project of Zhejiang Province (No. 2013C31068), the Applied Research Project of Zhejiang Provincial Education Department (Nos. Y201432598 and 201328587) and the China Postdoctoral Science Foundation funded project (No. 2014M551596).

References

1. N. Tripathi, L. D. Bell, S. Nikzad, and F. Shahedipour-Sandvik, Appl. Phys. Lett. **97**, 052107 (2010).
2. F. Machuca, Y. Sun, Z. Liu, K. Ioakeimidi, P. Pianetta, and R. F. W. Pease, J. Vac. Sci. Technol. B **20**, 2721 (2002).
3. J. Zhang, Y. Yang, and H. Jia, Chin. Opt. Lett. **11**, 102304 (2013).
4. Z. Liu, Y. Sun, P. Pianetta, J. R. Maldonado, R. F. W. Pease, and S. Schuetter, Appl. Phys. Lett. **90**, 231115 (2007).
5. H. Huang, D. Yan, G. Wang, F. Xie, G. Yang, S. Xiao, and X. Gu, Chin. Opt. Lett. **12**, 092301 (2014).
6. W. Siegmund, A. S. Tremsin, J. V. Vallerga, J. B. McPhate, J. S. Hull, J. Malloy, and A. M. Dabiran, Proc. SPIE **7021**, 70211B (2008).
7. Y. Shen, L. Chen, Y. S. Qian, Y. Y. Dong, S. Q. Zhang, and M. S. Wang, Appl. Surf. Sci. **324**, 300 (2015).
8. I. V. Bazarov, B. M. Dunham, X. Liu, M. Virgo, A. M. Dabiran, F. Hannon, and H. Sayed, J. Appl. Phys. **105**, 083715 (2009).

9. M. A. Moral, T. C. Sadler, M. Haberlen, M. J. Kappers, and C. J. Humphreys, Appl. Phys. Lett. **97**, 261907 (2010).
10. M. Higashiwaki, S. Chowdhury, B. L. Swenson, and U. K. Mishra, Appl. Phys. Lett. **97**, 222104 (2010).
11. W. Lim, J. H. Jeong, J. H. Lee, S. B. Hur, J. K. Ryu, K. S. Kim, T. H. Kim, S. Y. Song, J. I. Yang, and S. J. Pearton, Appl. Phys. Lett. **97**, 242103 (2010).
12. J. Stock, G. Hilton, T. Norton, B. Woodgate, S. Aslam, and M. Ulmer, Proc. SPIE **5898**, 58980F (2005).
13. L. Mizuno, T. Nihashi, T. Nagai, M. Niigaki, Y. Shimizu, K. Shimano, K. Katoh, T. Ihara, K. Okano, M. Matsumoto, and M. Tachino, Proc. SPIE **6945**, 69451N (2008).
14. W. Siegmund, J. S. Hull, A. S. Tremsin, J. B. McPhate, and A. M. Dabiran, Proc. SPIE **7732**, 77324T (2010).
15. F. S. Shahedipour, M. P. Ulmer, B. W. Wessels, C. L. Joseph, and T. Nihashi, IEEE J. Quantum Electron. **38**, 333 (2002).
16. J. L. Qiao, B. K. Chang, Y. S. Qian, X. Q. Du, Y. J. Zhang, and X. H. Wang, Proc. SPIE **7658**, 76581H (2010).
17. Y. S. Qian, B. K. Chang, J. L. Qiao, Y. J. Zhang, R. G. Fu, and Y. F. Qiu, Proc. SPIE **7481**, 74810H (2009).
18. X. H. Wang, B. K. Chang, L. Ren, and P. Gao, Appl. Phys. Lett. **98**, 082109 (2010).
19. X. H. Wang, B. K. Chang, Y. J. Du, and J. L. Qiao, Appl. Phys. Lett. **99**, 042102 (2011).
20. J. P. Perdew and A. Zunger, Phys. Rev. B **23**, 5048 (1981).
21. J. P. Perdew, K. Burke, and M. Ernzerhof, Phys. Rev. Lett. **77**, 3865 (1976).
22. M. D. Segall, P. J. D. Lindan, M. J. Probert, C. J. Pickard, P. J. Hasnip, S. J. Clark, and M. C. Payne, J. Phys. Condens. Matter **14**, 2217 (2002).
23. Y. J. Du, B. K. Chang, X. H. Wang, J. J. Zhang, B. Li, and M. S. Wang, Appl. Surf. Sci. **258**, 7425 (2012).
24. H. J. Monkhorst and J. D. Pack, Phys. Rev. B **13**, 5188 (1976).
25. J. Perdew, Phys. Rev. Lett. **77**, 3865 (1996).
26. S. Krukowski, P. Kempisty, and P. Strak, J. Appl. Phys. **105**, 113701 (2009).
27. P. Perlin, C. Jauberthie-Carillon, J. P. Itie, A. San Miguel, I. Grzegory, and A. Polian, Phys. Rev. B **45**, 83 (1992).
28. W. E. Spicer and A. Herrera-Gómez, Proc. SPIE **2022**, 18 (1993).
29. A. L. Rosa and J. Neugebauer, Phys. Rev. B **73**, 205346 (2006).
30. H. Tsuda and T. Mizutani, Appl. Phys. Lett. **60**, 1570 (1992).
31. X. Q. Du and B. K. Chang, Appl. Surf. Sci. **251**, 267 (2005).
32. Y. S. Qian, Z. Y. Zong, and B. K. Chang, Proc. SPIE **4580**, 486 (2001).
33. B. K. Chang, X. Q. Du, L. Liu, Z. Y. Zong, R. G. Fu, and Y. S. Qian, Proc. SPIE **5209**, 209 (2003).
34. F. Machuca, "A thin film p-type GaN photocathode: prospect for a high performance electron emitter," Ph.D. dissertation (Stanford Univeristy, 2003).
35. D. Durek, F. Frommberger, T. Reichelt, and M. Westemann, Appl. Surf. Sci. **143**, 319 (1999).
36. Y. J. Zhang, J. J. Zou, X. H. Wang, B. K. Chang, Y. S. Qian, J. J. Zhang, and P. Gao, Chin. Phys. B **20**, 048501 (2011).